PHYSICAL REVIEW E **84**, 045302(R) (2011)

Self-organization of hydrogen gas bubbles rising above laser-etched metallic aluminum in a weakly basic aqueous solution

E. V. Barmina, P. G. Kuzmin, and G. A. Shafeev

Wave Research Center, A. M. Prokhorov General Physics Institute, Russian Academy of Sciences, 38 Vavilov Street, 119991 Moscow, Russia

(Received 8 June 2011; revised manuscript received 31 August 2011; published 10 October 2011)

Self-organization of hydrogen bubbles is reported under etching of metallic Aluminum in a weakly basic solution. The ascending gas bubbles drift to the areas with higher density of bubbles. As a result, ascending bubbles form various stationary structures whose symmetry is determined by the symmetry of the etched area. Bubbles are aligned along the bisectors of the contour of the etched area. The special laser-assisted profiling of the etched area in shape of a vortex induces a torque in the fluid above the etched area. The process is interpreted on the basis of Bernoulli equation.

DOI: 10.1103/PhysRevE.84.045302 PACS number(s): 47.20.Bp, 47.55.D−, 82.45.−h, 82.50.Hp

Introduction. The formation of dissipative structures is typical for open systems. A system organizes itself so as to minimize local entropy production in the generalized direction of the applied force [1]. Liquid flow in the field of gravity is characterized by a number of instabilities, e.g., Rayleigh-Bénard instability or Bénard-Marangoni convection. In some cases these instabilities lead to the formation of self-organized structures like the well-known Bénard cells that appear due to buoyancy force. The self-organized structures arise as the result of amplification of microscopic fluctuations to a macroscopic level through bifurcation. The addition of small solid particles to the liquid is largely used for visualization of hydrodynamic flows. For example, fine aluminum powder (flakes) can be used to visualize either Bénard cells or Marangoni convection flows [2]. Sufficiently small solid particles that do not interact with each other are believed to be tracers of liquid flows. However, it was found that the suspended particles form their own trajectories in the conditions of Marangoni convection [2,3]. The particles are ordered in a symmetric closed trajectory that rotates at certain angular velocity. The explanation of this fact has been given in a recent paper [4]. The deviation of particle trajectories from the hydrodynamic flow is due to their inertia. The resulting trajectory is the interplay between viscous drag forces and inertial behavior of particles motion.

Another example of a two-phase system is a fluid with gas bubbles. Bubbly flows with a large bubble concentration occur in many natural and industrial processes, for example, in propeller-induced cavitation in ship building, cavitation in fluid machinery, nucleate boiling in reactors and similar devices, and many processes (centrifuges, mixers) in the chemical process industry. Purging gas bubbles is widely used in practice (so-called flotation) for the purification of water from oil and minerals [5], water ozonation, etc. *A priori*, gas bubbles can hardly be considered as tracers of hydrodynamic flows. In the field of gravity their motion is dominated by the buoyancy force, which is compensated by the viscous Stokes force at the bubble-liquid interface. Small (100–200 μm in diameter) individual bubbles demonstrate the instability of their shape upon rising in water. Moreover, individual small bubbles rise rectilinearly, while larger bubbles follow a zigzag trajectory [6]. Rising bubbles can interact with each other, and when a pair of bubbles rises in a still liquid due to buoyancy, the bubbles are attracted toward (repelled from) each other when the angle between their line of centers and the vertical direction is inside (outside) the range $[\theta_c, 180^\circ - \theta_c]$, with θ_c being a critical angle ranging from 35° when the two bubbles are in contact to 54° when they are widely separated [7]. The adjacent bubbles interact with each other through vorticity fields around them. The switching of bubble behavior occurs at some critical Reynolds number. Sufficiently close bubbles form a horizontal cluster that rises vertically with their line of centers being perpendicular to the rise velocity [8]. Large (4–5 mm) bubbles tend to form a vertical cluster [9]. The type of clustering depends on the deformability of the bubbles. According to Bernoulli's equation, higher fluid velocity in the wake of a bubble results in lower pressure, and the second bubble is shifted underneath. The rising of gas bubbles at high concentration (20% or more) in the fluid is a collective effect and may cause the fluid to flow due to viscous interaction. In turn, the liquid flow affects the motion of the bubbles, so there is a feedback between the flows of the liquid and the concentration of gas bubbles. Therefore, this positive feedback may lead to the formation of dissipative structures made of gas bubbles.

In this Rapid Communication we report a type of ordering of gas bubbles rising under etching of an aluminum plate in a weak basic solution. The self-organization of emerging hydrogen bubbles can easily be observed due to light scattering. This phenomenon is generic and appears in different chemical processes in liquid phase that are accompanied by the emission of gas bubbles [10]. The aqueous solution of ammonia is a weak base, and its interaction with Al results in hydrogen emission. After a certain incubation period of time, the bubbles are aligned into a stationary pattern according to the geometry of the etched area. Namely, hydrogen bubbles find the bisectors of polygonal laser-processed areas. The special laser-assisted profiling of the etched area in the shape of a vortex induces a torque in the fluid above the laser-processed area without any mechanical stirring.

Experimental results. Gas bubbles appear during the reaction of laser-treated areas of a bulk aluminum target with a 5% concentration. Laser exposure of the target in air leads to the formation of a surface with high specific area [10]. A raster scan of the laser beam over the Al plate allows the

FIG. 1. (Color online) Side view of hydrogen bubble distribution under etching of a laser-processed Al target. The lateral size of the laser-treated area is 1 cm. The dark line on the target is the edge of the laser-exposed area.

generation of arbitrary shapes of the treated areas, e.g., square or triangle. The exposed areas look dark compared to the initial substrate due to multiple reflections of light in the laser-induced microstructures. This provides a dark background for observations of bubble patterns. Upon immersion in the etching solution, the microbubbles of hydrogen are generated mostly in laser-processed areas of the substrate. After some incubation time of several minutes etching of the aluminum starts and is accompanied by emission of microbubbles of hydrogen with a diameter between 100 and 200 μm, as measured by a horizontal microscope.

Figure 1 shows that the distribution of gas bubbles that is established in the bubbly flow over the laser-treated area of Al plate after some incubation time is not homogeneous (Fig. 1). Gas bubbles produced at the periphery of the laser-treated area move to its center with simultaneous rising. They drag the liquid and disappear at the surface, while the liquid flows horizontally, reaching the vessel walls, and then descends. We did not observe zigzag trajectories of bubbles in our experimental conditions, which is due to their small size. Apparently, the bubble keeps its spherical shape due to the weak perturbations from the detachment during etching. Some bubbles probably form clusters in the central part of the bubbly flow; however, they cannot be resolved as individual objects due to high density.

The chemical interaction of metallic aluminum with the etchant may lead to a temperature increase in the substrate. In our experimental conditions, however, this temperature difference is small, and a stationary regime of etching does not exceed a few Kelvin. The length of the tracks of gas bubbles during the shutter exposure allows estimating the velocities of the flows in various regions of the solution. In the bubbles-rich area the rising velocity is around 5 mm/s [10]. This corresponds to a Reynolds number (based on the bubble diameter and rise velocity) of $\sim$1.

One can see that the lateral size of a bubble-rich area near the interface of fluid and air is noticeably narrower than that of the laser-treated area on the target from which the bubbles are emitted. This might be attributed to the drag of bubbles by flows at the vessel bottom. However, further observations indicate that this is not the case.

The self-organization of hydrogen bubbles is easily observed from the top. The dark background of the laser-processed area is especially helpful. The top view of the etched Al target shows the formation of patterns made of gas bubbles. A pattern appears at sufficiently large thickness of the liquid above the laser-etched area (Fig. 2), and the bubbles are aligned along diagonals of the square area.

At small thickness of the liquid the bubbles are distributed homogeneously over the laser-treated area of the target [Fig. 2(a)]. The bubbles scatter incident light and can be observed over the dark background of the etched Al as bright areas. At higher thickness the gas bubbles are aligned along the diagonals of the square [Fig. 2(b)]. Note that the symmetry of the pattern is completely different from the symmetry of the vessel (round Petri dish). The structure formed by gas bubbles is stationary and very stable. It remains the same at least for 2 h of etching until the etching solution is exhausted.

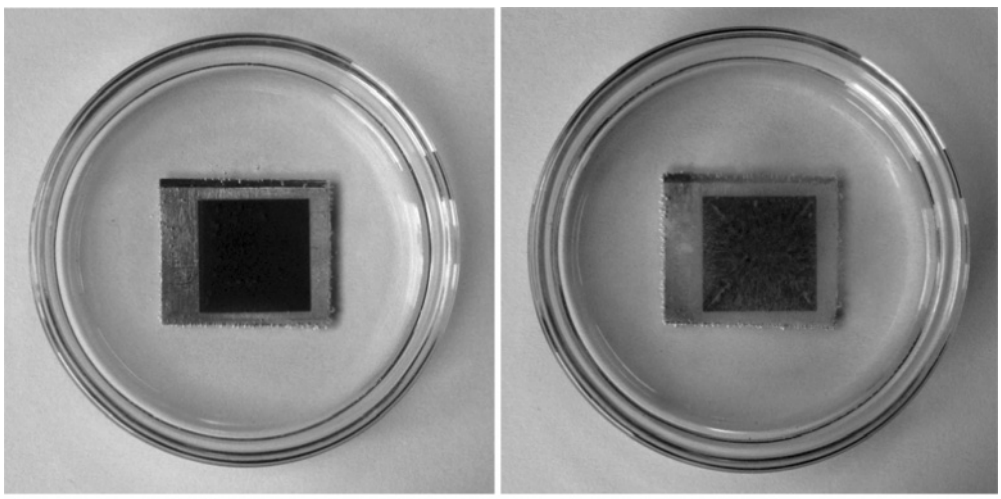

(a) (b)

FIG. 2. Stationary pattern of gas bubbles over the square-shaped laser-treated area of the aluminum target. (a) Thickness of the liquid of 0.4 mm, stationary pattern; (b) thickness of 5 mm. The size of the laser-scanned square is 15 $\times$ 15 mm^2. Top view is shown; the concentration of NH_4OH is 5%.

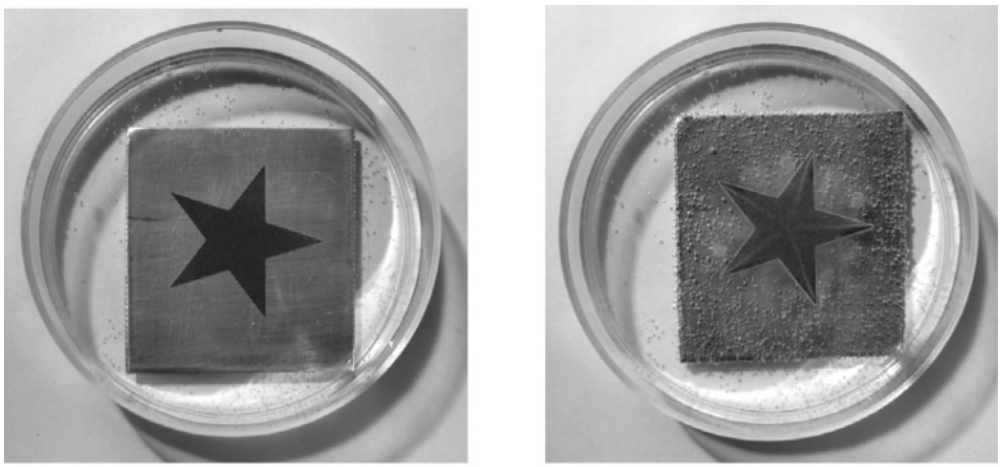

(a) (b)

FIG. 3. Formation of the pattern of gas bubbles over a star-shaped laser-processed area. (a) Onset of etching; (b) stationary pattern. The size of the star-shaped etched area is 15 mm.

The stationary pattern formed by gas bubbles in the case of a starlike laser-processed area is presented in Fig. 3. At the onset of etching the gas bubbles that rise toward the surface of the liquid form a star-like pattern [Fig. 3(a)]. Then the bubbles are aligned along the rays of the star-shaped etched area. There are few bubbles on the nontreated area of the target, which facilitates the observation of the pattern above the etched area.

Finally, if the etched area has the shape of an arbitrary triangle, the gas bubbles are aligned along the bisectors of the triangles, as demonstrated in Fig. 4. Some deviation from bisectors is due to the tilt of the camera.

If the laser-etched area has the specific vortex shape shown in Fig. 5, then the entire liquid above the target starts rotating. The rotation is visualized both by spiral trajectories of rising bubbles and by microscopic pieces of etched aluminum detached from the laser-processed area that have neutral buoyancy in the etching solution. In this case, however, the thickness of the liquid layer above the target should be at least of several centimeters. Each bubble has the velocity component toward the center and also a tangential component according to the curvature of the "petals" of the laser-etched vortex. For a 4-cm vessel, the angular velocity of fluid rotation is about 1 rpm.

It is clear that the laser here generates only the shape of the preferably etched area. Similar results could be obtained if the shape of the Al plate coincided with the configuration of the laser-treated area, either in the shape of a square or a star.

An individual gas bubble rises with constant velocity due to the action of two forces, namely, the Stokes viscous force and the buoyancy Archimedes force due to the low density of the gas inside it. Each gas bubble drags the surrounding liquid into ascending motion. If the density of the bubbles on both sides of the bubble is different, then the velocity of the liquid

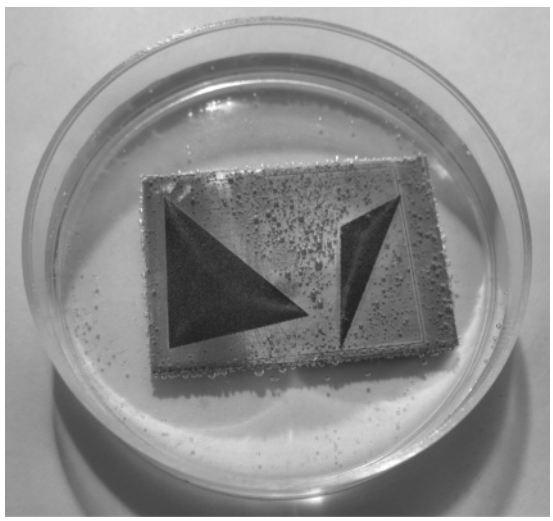

FIG. 4. Stationary pattern of gas bubbles over triangle-shaped areas. The bubbles are aligned along the bisectors of the triangle.

FIG. 5. Macroview of a special vortex pattern of a laser-processed area of an aluminum plate that causes stationary rotation of the liquid in the whole vessel. The diameter of the laser-treated area is 20 mm. The direction of rotation is counterclockwise.

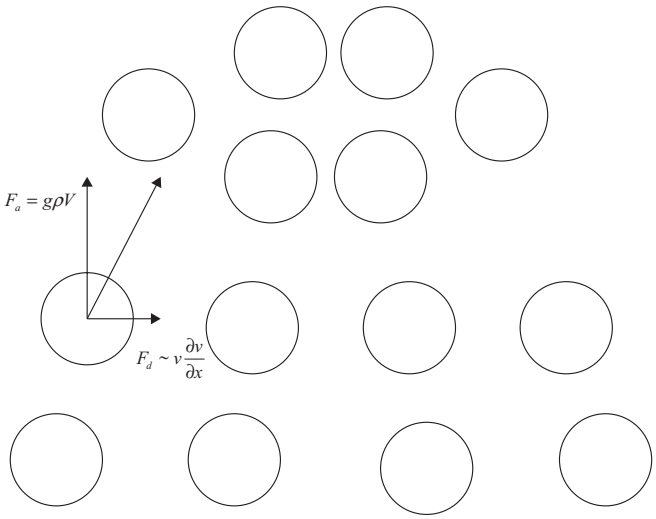

FIG. 6. Forces that determine the bubbles' motion: F_a, buoyancy force; F_d, drift force.

on both sides of the bubble is also different (Fig. 6). The higher the bubble concentration is, the higher the bulk velocity of the fluid is. According to the Bernoulli equation, higher velocity corresponds to lower pressure. Therefore, a drift force appears that moves the bubble toward the region of higher velocity of the fluid flow. Therefore, the rising bubble drifts to the flow center, increasing thus the velocity of this flow. This is the positive feedback that governs the formation of a pattern of gas bubbles. There is a difference of pressure between the left and right sides of a bubble since the velocity of liquid flow is related to the local density of rising bubbles. This pressure difference causes a bubble to drift to the area with the higher density of bubbles.

The necessary condition for observations of patterns formed by gas bubbles is $h/a \leqslant 1$, where h is the height of the liquid layer above the etched area. The pattern is smeared at $h/a > 1$, as seen in Fig. 1, and is not visible from the top due to screening by rising bubbles. The formation of the bubble pattern is suppressed at $h \ll a$ [Fig. 2(a)] since bubbles disappear at the surface of the liquid before their significant drift to the center of the flow may occur.

The formation of dissipative structures described in the present work is due to the positive feedback between the bubble motion and liquid flows around it. The source of energy needed for bubble rearrangement is the chemical reaction between the metal and the surrounding solution. Figure 7 shows the

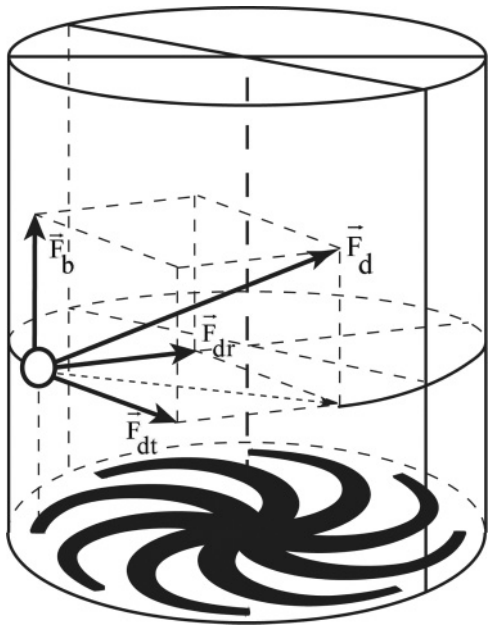

FIG. 7. Forces applied to a gas bubble in the case of a vortex-like shape of the laser-ablated area. F_b, buoyancy force; F_d, drift force.

forces that affect the gas bubble over a vortex-like area. For a bubble situated at the periphery of a petal the maximum density of bubbles is situated on the nearest petal. In this case the drift force F_d has both radial (F_{dr}) and tangential (F_{dt}) components since the higher concentration of gas bubbles over the vortex-shaped area is shifted from the center for each peripheral bubble.

Thus, a type of self-organized structures has been described. The structures are formed by falling hydrogen bubbles that are emitted during chemical reaction of a metal with an ammonium solution. The mechanism of formation of such patterns is ubiquitous and is stipulated by the positive feedback between bubble concentration and flows through viscous interaction. The successful observation of the self-organization of bubbles is due to the unique combination of the technique of laser-assisted processing of metals with relatively slow chemical etching of aluminum. A similar phenomenon is also observed under etching of laser-processed Al with aqueous solutions of either NaOH or KOH, as well as during etching of laser-exposed Si wafers in HF acid [11]. It is believed that the effect of self-organization of gas bubbles may find a number of practical applications.

[1] I. Prigogine, *Introduction to Thermodynamics of Irreversible Processes*, 2nd ed. (Wiley, New York, 1961).

[2] D. Schwabe, A. I. Mizev, M. Udhayasankar, and S. Tanaka, Phys. Fluids **19**, 072102 (2007).

[3] D. Schwabe, P. Hintz, and S. Frank, Microgravity Sci. Technol. **9**, 163 (1996).

[4] D. O. Pushkin, D. E. Melnikov, and V. M. Shevtsova, Phys. Rev. Lett. **106**, 234501 (2011).

[5] M. R. Beychok, *Aqueous Wastes from Petroleum and Petrochemical Plants* (Wiley, New York, 1967).

[6] M. Wu and M. Gharib, Phys. Fluids **14**, L49 (2002).

[7] D. Legendre, J. Magnaudet, and G. Mougin, J. Fluid Mech. **497**, 133 (2003).

[8] L. van Wijngaarden, J. Fluid Mech. **251**, 55 (1993).

[9] J. Martinez Mercado, D. Chehata Gomez, D. van Gils, C. Sun, and D. Lohse, J. Fluid Mech. **650**, 287 (2010).

[10] M. E. Shcherbina, E. V. Barmina, P. G. Kuzmin, and G. A. Shafeev, e-print arXiv:1105.4957.

[11] V. V. Voronov, S. I. Dolgaev, S. V. Lavrischev, A. A. Lyalin, A. V. Simakin, and G. A. Shafeev, Appl. Phys. A **73**, 177 (2001).